Zernike generation with MEMS deformadle mirror actuated by electrostatic piston array

AUTHOR(S):

Uno, Akiko; Hirai, Yoshikazu; Tabata, Osamu; Tsuchiya, Toshiyuki

CITATION:

Uno, Akiko ...[et al]. Zernike generation with MEMS deformadle mirror actuated by electrostatic piston array. 2018 IEEE Micro Electro Mechanical Systems (MEMS) 2018: 704-707

ISSUE DATE:

2018

URL:

http://hdl.handle.net/2433/284803

ZERNIKE GENERATION WITH MEMS DEFORMABLE MIRROR ACTUATED BY ELECTROSTATIC PISTON ARRAY

Akiko Uno, Yoshikazu Hirai, Osamu Tabata and Toshiyuki Tsuchiya
Department of Micro Engineering, Kyoto University, Kyoto, JAPAN

ABSTRACT

We report a low-voltage and large-displacement electrostatic deformable mirror for *in vivo* retinal imaging by adaptive-optics optical coherence tomography. The mirror utilizes an electrostatic piston actuator which allows bottom electrodes to move vertically to keep the gap small to maintain large actuation force at low actuation voltage. An 8-mm-diameter mirror device was fabricated from two components; the mirror part and the actuator part. The parts were assembled with 7-µm-gap defined by an SU-8 layer. We successfully demonstrated operation of the mirror in various Zernike modes.

INTRODUCTION

MEMS deformable mirrors (MEMS-DMs) are used in compact adoptive optics to improve image resolutions in optical coherence tomography for retinal imaging and endoscopic optical biopsy [1]. An electrostatically actuated MEMS-DM has a simple structure and is fabricated relatively easily [2]. However, electrostatic actuation has a problem of its high actuation voltage for large deformation, compared to piezoelectric [3] and electromagnetic actuation [4]. In a commercially available electrostatic deformable mirror device, 200-250 V actuation voltage is required for a few micrometers stroke, since the electrostatic force decreases by square of gap distance. For solving this problem, we have proposed an electrostatic piston structure, in which the bottom electrode of the parallel plate actuator, which is fixed in a conventional DM device, can move vertically by following mirror plate deformation. We have verified 6-µm stroke at 60 V for astigmatism mode deformation by finite element analysis [5] and have demonstrated preliminary operation of the fabricated MEMS-DM [6] for a proof of concept. In this report, in order to examine the performance of the proposed DM as a wave-front compensation device, various wave-front shapes were actuated and the generated shapes were analyzed with Zernike polynomials.

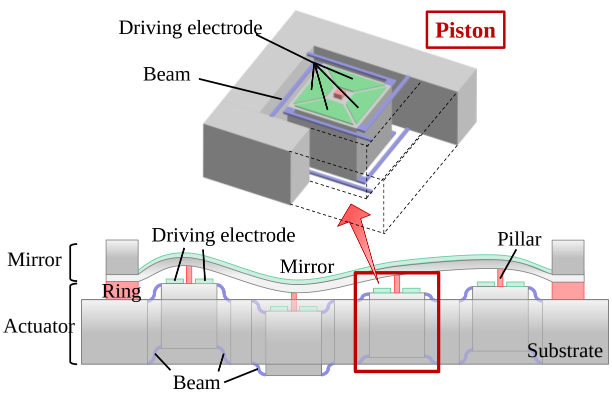

Figure 1: Device schematics of deformable mirror actuated with electrostatic piston array.

DEFORMABLE MIRROR

Operation principle

The schematic drawing of the proposed mirror is shown in Fig 1. The mirror consists of two parts; the mirror part on the top and the actuator mirror part at the bottom. The mirror part has a thin deformable mirror plate (2-µm thick and 8-mm in diameter) acting as a moving electrode. On the actuator part, there is an array of suspended silicon blocks (called piston) which is allowed to move vertically. To avoid lateral and tilting motions of the piston, it has four beams on each (top and bottom) surface arranged in a spiral shape. Each piston has four driving electrodes around a pillar at the center. The pillar defines a gap between the mirror plate and the driving electrodes. The mirror is actuated electrostatically by applying the voltage between them. The actuation force causes the tilting motion of the plate with respect to the contact point of the pillar as a fulcrum. The vertical motion of the mirror plate is determined by the superposition of the motions generated by all pistons. For example, when the electrodes placed outside in each piston with respect to the center of the mirror are actuated, the mirror deforms convex shape, whereas the inner electrode actuation causes concave deformation as shown in Fig. 2. The convex deformation that has been thought to be difficult to be presented with electrostatic DMs can be generated by arraying the pistons. In addition, the pistons move vertically with following the motion of the mirror plate, so that the gap between the electrodes is maintained small because of the pillar. It is useful to make actuation force always sufficient and to avoid stiction.

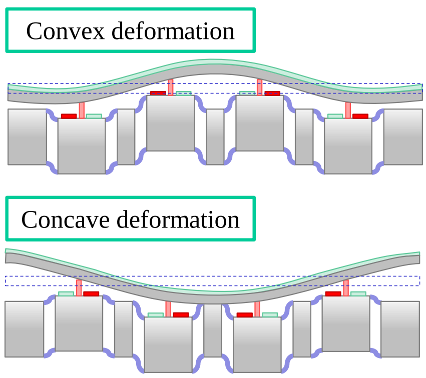

Figure 2: Operation principle. By applying voltages on RED colored electrodes, convex (upward) and concave (downward) deformations are presented.

Device design and fabrication

The mirror part (Figs. 3) was fabricated from silicon-on-insulator (SOI) wafer with 2-µm-thick device layer with simple back-side removal process using DRIE (Fig. 4). The silicon mirror plate was covered with aluminum from bottom for a reflection layer and chromium from top for stress control. The fabricated mirror part is

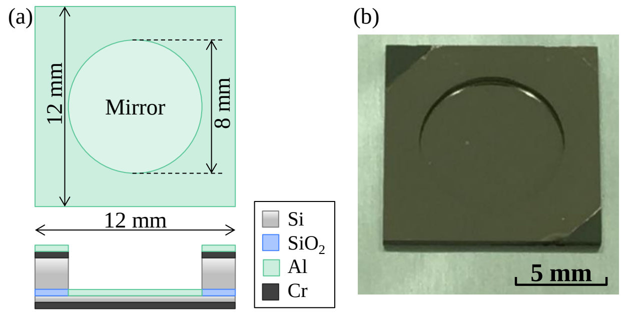

Figure 3: Mirror part; a) design and b) fabricated.

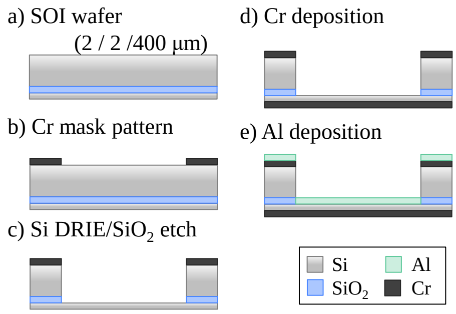

Figure 4: Fabrication process of mirror part.

shown in Fig. 3b. Because of its large diameter and thinness, the mirror plate tends to buckle from the internal stress of the device layer silicon film. By adding the chromium layer of 15-nm, the flat mirror at initial state was realized.

A design of the actuator part is shown in Fig. 5. In this specific design, there are fifteen pistons arranged concentrically. The sixty driving electrodes are connected to the wiring pads at the edges of the 16-mm-square chip. The part was fabricated from a double-side-polished (DSP) silicon wafer covered with thermal oxide and LPCVD low-stress silicon nitride films as shown in Fig. 6. The pistons are supported by four beams of the low-stress nitride arranged to spiral shape on each side of the wafer. The electrodes and wirings are made by aluminum. Thermal oxide film and the plasma CVD oxide film deposited using tetraethyl orthosilicate (TEOS) are used for passivating the aluminum and nitride films during silicon etching steps. An SU-8 layer of 7-μm thick was patterned to form the piston and the spacer (called as ring) to determine the gap. Then, the trenches that define the shape of piston were etched by the Bosch process using ICP-RIE for the depth of 175-μm from the both sides. The remaining 50-μm thick silicon was etched isotropically using XeF_2, which causes undercutting and the silicon substrate under the beams were removed to release the pistons. This process steps enables us to fabricate the suspending beams on both sides without using wafer bonding process. The fabricated actuator part and the scanning electron micrograph of the piston are shown in Fig. 7. The total layer structure of the DM is shown in Table 1.

RESULTS AND DISCUSSIONS

The fabricated actuator and mirror parts were assembled by just stacking two parts without any bonding process. To align two parts and make electrical connection

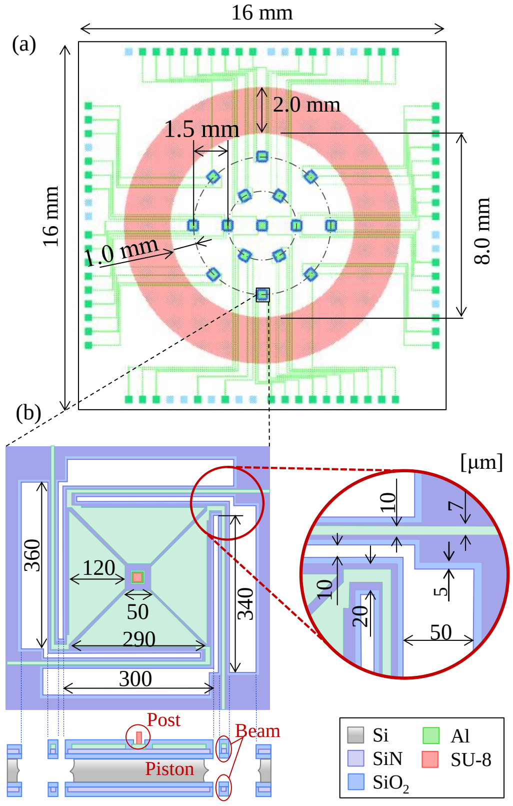

Figure 5: Actuator part design. a) photomask design of 15 pistons type. b) schematic drawings of piston.

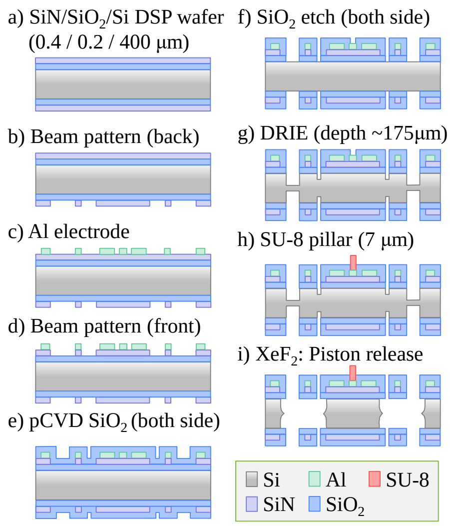

Figure 6: Fabrication process of actuator part.

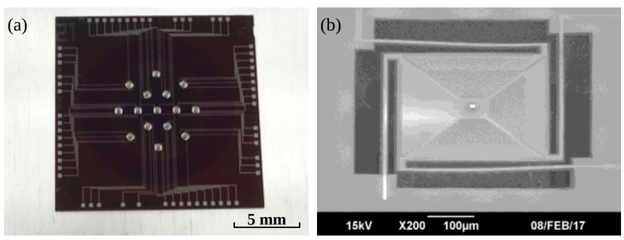

Figure 7: Fabricated actuator part. a) chip. b) piston.

for driving, a custom designed socket was prepared. The socket was designed to fit the both parts placed with good alignment accuracy and has pins to make electrical

Table 1: Layers structure of electrostatic piston array.

Part	Layer	Material	Thickness
Mirror	Substrate	Si	400 µm
	Insulator	SiO_2	2 µm
	Reflection	Al	0.2 µm
	Membrane	Si	2 µm
	Stress control	Cr	15 nm
Piston	Spacer (Pillar, Ring)	SU-8	7 µm
	Electrode	Al	0.2 µm
	Passivation	TEOS	0.5 µm
	Beam (top)	LS-SiN	0.4 µm
	Passivation	Th-SiO_2	0.2 µm
	Substrate	Si	400 µm
	Passivation	Th-SiO_2	0.2 µm
	Beam (bottom)	LS-SiN	0.4 µm
	Passivation	TEOS	0.5 µm

connection to the pads (Fig. 8). The sixty driving electrodes on the fifteen pistons are driven individually using two 32-ch 13bit DA convertor boards (PXI-6723, National Instruments) and a custom-made PCB with sixteen 4ch high-voltage amplifiers (HV264TS-G, Microchip). The output voltage is controlled by a PC with its range from 0 to 200V. The deformation of DM was measured using a small aperture interferometer (PTI250, Zygo). Although the mirror plate was very flat before assembly, it has astigmatism deformation of about 0.5-µm due to stress induced by insertion to the socket. The deformations reported below were difference from the initial deformation after assembly.

Figs. 9 show the deformations for displaying typical Zernike polynomial modes (tilt, astigmatism, spherical and trefoil). The voltage application patterns are shown in the figures. Though the voltage application pattern has not been optimized, each mode of deformation was displayed as we designed. However, the deformation (peak-to-peak) was less than 0.25 µm which is much smaller compared to the finite-element simulation results. In addition, the upward displacement looks smaller than the downward,

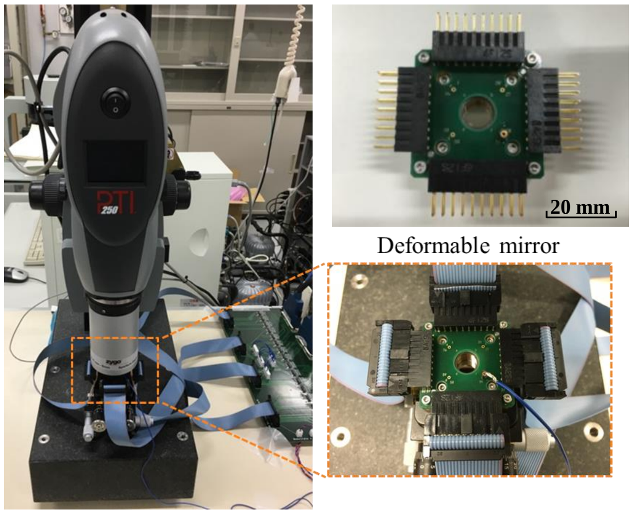

Figure 8: Experimental set-up using interferometer. Assembled mirror device to custom made socket. Mirror plate is seen at center hole of PCB.

which can be identified by the fact that the edge of the mirror has almost highest position. The tilt and astigmatism modes display their mode well, but the trefoil and spherical modes seem to contain other modes. We analyzed the deformation using Zernike polynomial decomposition. Figs. 10 show the Zernike coefficient of each deformation modes. We can find that the largest component is the mode that we intend to display and the proposed electrostatic piston array can display complicated deformation. In the current piston arrangement, the trefoil mode has a tetrafoil component and the spherical mode also has higher order spherical components. Both of them would be caused by the arrangement of the pistons, therefore, optimization of the arrangement to display various modes with a minimum error is required.

In this experiment, we expected that each electrode on the piston should generate the deformation with large curvature on the mirror plate, but the generated deformation looks localized, only near the piston. The reason would be the in-plane tension force of the mirror

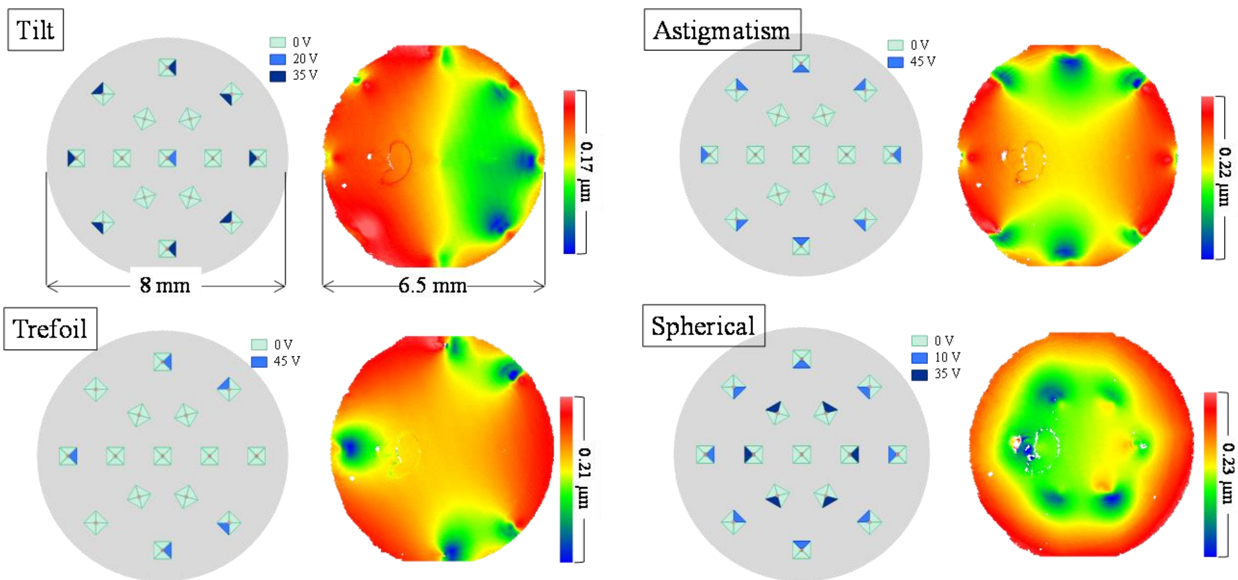

Figure 9: Generated mirror deformations (image on right) with applied voltage pattern indicated in drawing on left.

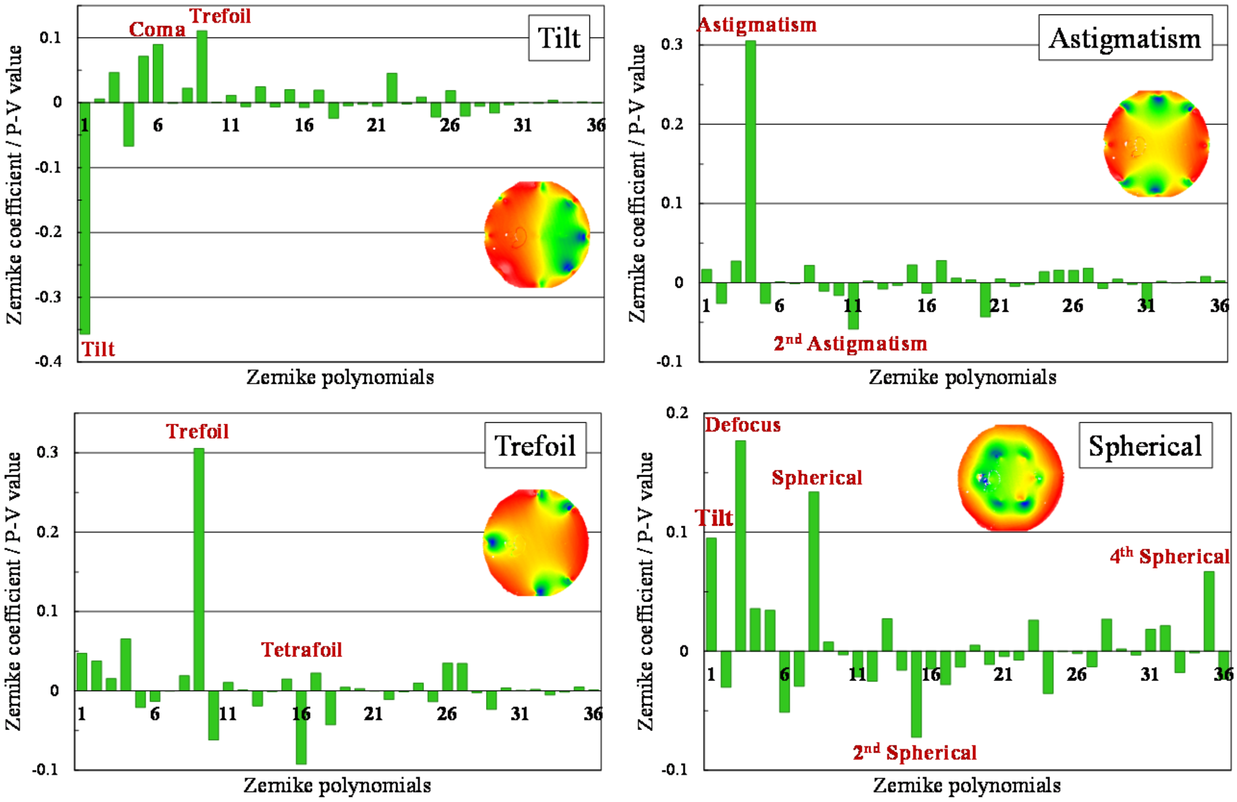

Figure 10: Generated mirror deformations decomposed to Zernike polynomials up to mode 36.

plate caused by the internal stress and the hardening effect due to large deformation. Optimization of the layer structure, such as the thickness of the metal films and silicon film and the application of different materials (such as silicon nitride or polymer film) instead of silicon will be needed, as well.

CONCLUSION

The presentation of Zernike polynomial mode deformation was demonstrated using the MEMS-DM with the electrostatic piston array. Because of the pistons that moved vertically to make the capacitance gap constant, low voltage operation was realized. We have confirmed that the MEMS-DM generated 1) deformation of about 0.2 μm with relatively low voltage (<50V), 2) concave (upward) deformation and 3) generation of Zernike modes up to 3rd order with the simple piston arrangement. Adaptive optics system with the DM is going to be realized by developing the mathematical model and control system to express the deformation against applied voltages. To increase the deformation and to express higher order Zernike modes, the optimization of thickness and material of the mirror plate and arrangement of the pistons should be investigated.

ACKNOWLEDGEMENTS

A part of this work was supported by the "Nanotechnology Platform Japan" Program (Nanotechnology Platform, Kyoto University).

REFERENCES

[1] D. J. Dagel, W. D. Cowan, O. B. Spahm, G. D. Grossetete, A. J. Griñe, M. J. Shaw, P. J. Resnick. B. Jokiel, "Large-Stroke MEMS Deformable Mirrors for Adaptive Optics," *J. Mircoelectromech. Syst.* Vol. 15, pp. 572-583, 2006.

[2] M. Horenstein, T. Bifano, S. Pappas, J. Perreault, R. Krishanamoorthy-Mali, "Real time optical correction using electrostatically actuated MEMS devices," *J. Electrostatics*, Vol. 46, pp. 91-101, 1999.

[3] I. Kanno, T. Kunisawa, T. Suzuki, H. Kotera, "Development of deformable mirror composed of piezoelectric thin films for adaptive optics," *IEEE J. Sel. Top. Quant. Electron.*, Vol. 13, pp. 155-161, 2007.

[4] O. Cugat, S. Basrour, C. Divoux, P. Mounaix, G. Reyne, "Deformable magnetic mirror for adaptive optics: technological aspects," *Sens. Actuators A: Physical*, Vol. 89, pp. 1-9, 2001.

[5] T. Tsuchiya, V. K. Singh, Y. Hirai, O. Tabata, "Large-displacement electrostatic deformable mirror with movable bottom electrodes," in *Proc. Optical MEMS and Nanophotonics (OMN2014)*, Glasgow, Scotland, August 17-21, 2014, pp. 119-120.

[6] A. Uno, Y. Hirai, T. Tsuchiya, O. Tabata, "Fabrication of MEMS Deformable Mirror Actuated by Electrostatic Piston Array," in *Proc. Optical MEMS and Nanophotonics (OMN2016)*, Singapore, July 31-August 4, 2016, pp. 55-56.

CONTACT

*T. Tsuchiya, tel: +81-75-383-3691;
tutti@me.kyoto-u.ac.jp